Catalytic Hydrogenation of Hemicellulosic Sugars: Reaction Kinetics and Influence of Sugar Structure on Reaction Rate

Victoria D.S. Freitas,[a] Ana Paez,[a] Pascal Fongarland,[a] Régis Philippe,[a] Léa Vilcocq*[a]

[a] Dr V.D.S. Freitas, A. Paez, Pr P. Fongarland, Dr R. Philippe, Dr L. Vilcocq*
Univ Lyon, CNRS, UCBL, CPE-Lyon, CP2M – UMR 5218, F-69616 Villeurbanne, France
E-mail: lea.vilcocq@cnrs.fr

Supporting information for this article is given via a link at the end of the document.

Abstract: Hemicelluloses are a major component of lignocellulosic biomass. Different sugars can be obtained from hemicelluloses: xylose, arabinose, galactose, mannose, glucose. Their catalytic hydrogenation produces polyols: xylitol, arabinitol, dulcitol, mannitol, sorbitol, which are valuable chemicals and platform molecules. In this paper, the hydrogenation of sugars was investigated with a Ru/TiO_2 catalyst. The influence of temperature, pressure, xylose concentration and catalyst amount was studied for xylose hydrogenation and a Langmuir-Hinshelwood kinetic model was designed. The comparative study of five hemicellulose sugars showed a strong impact of sugar structure on hydrogenation rate: hexoses (glucose, mannose, galactose) react slower than pentoses (xylose, arabinose).

Introduction

Biomass is the only abundant renewable source of carbon for chemicals.[1,2] With the incentive of climate change mitigation and reduction of dependence on oil-based resources, the importance of bioeconomy and bio-based chemistry is gaining importance worldwide[3,4] and particularly in Europe: the European market of bio-based chemicals has recently been estimated at c.a. 177 bn €. For 2030, the target of European Green New Deal has been set at 25% of bio-sourcing in chemistry.[5]

Among various sources, lignocellulose is the most promising terrestrial and non-edible biomass. It represents the major part of fibrous plants (e.g. trees, grasses, straws). Lignocellulose is a composite material constituted of three biopolymers: cellulose (40-60%), a gluco-polysaccharide; hemicelluloses (20-40%), which are hetero-polysaccharides; and lignin (15-40%), an aromatic- and phenolic-based biopolymer.[6] Therefore, hemicelluloses are major components of lignocellulose. Their valorisation can play a major role in the future development of biorefineries.

Hemicelluloses tether cellulose microfibrils in the cell walls of plants and strengthen them. They present a large variety of polymeric structures (e.g. linear, branched) and of monomer units (hexoses, pentoses, acetyl groups, aldonic acids). They are usually categorized in different types according to their sugar composition: xylans, mannans, β-glucans, xyloglucans, galactans, arabinans and arabinogalactans.[7,8] Several hemicelluloses types can be present in a plant in various proportions: xylans are predominant in hardwoods, mannans in softwoods, xylogulcans in grasses.

Five sugars are present in hemicelluloses: two pento-aldoses, xylose and arabinose; and three hexo-aldoses, glucose, mannose and galactose (Scheme 1). With the exception of glucose, all these sugars are found exclusively in hemicelluloses. They can be produced by hydrolysis with enzymatic catalysts or with mineral acids.[9,10] Heterogeneous catalysts have also been investigated for this reaction.[11,12]

The reduction of hemicellulose sugars leads to the corresponding polyols: xylitol, arabitol, sorbitol (from glucose), mannitol, dulcitol (from galactose) (Scheme 1). Sorbitol and mannitol are produced at industrial scales by catalytic hydrogenation of glucose or inverted sugar (hydrolysed sucrose, i.e. mixture of glucose and fructose). Xylitol is produced industrially by catalytic hydrogenation of xylose coming from xylan (from birch or corncob).[13] Xylitol market in 2016 was estimated c.a. 190 kt/year.[14] Polyols have a high added value in pharmaceutical and agro-food industries as low-calories sweeteners and additives (sorbitol = E420; mannitol = E421; xylitol = E967).[13] Because they do not have any petrochemical alternatives, polyols can also be interesting building blocks for organic synthesis, and as such, xylitol and sorbitol have been included in several reports on the most promising molecules from biomass.[15,16] They can also be used in polymers manufacturing.[14]

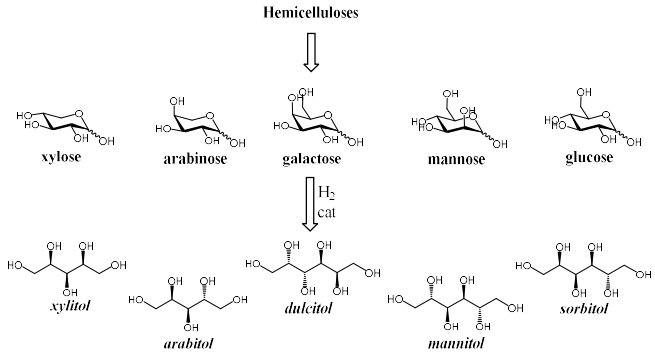

Scheme 1. Hydrogenation of ex-hemicelluloses sugars.

Catalytic hydrogenation of sugars is an industrial process but to our surprise, literature on hydrogenation catalysts for sugars other than glucose and, to a lesser extent, xylose, is rare.

Xylose and glucose hydrogenation has been studied with metal supported catalysts. Historically, Ni Raney has been applied for polyol production; however, nickel leaching led to contamination issues for food applications. Among noble metals, Ru was the most active for the conversion of sugars into polyols in literature.[17] It surpassed the performances of other notable metals such as Ni, Rh, Pt and Pd.[17–19] Bimetallic PtSn catalysts have also been proposed.[20] Besides, Co catalyst has recently been proposed as an alternative to noble metals for xylose hydrogenation.[21] Due to their good resistance to hydrothermal conditions, the activated carbon and titanium dioxide are good support candidates for sugars hydrogenation.

Few publications have compared the reactivity of different hemicellulosic sugars during hydrogenation. It was observed in a few rare studies that sugar structure could influence the hydrogenation reactivity. Zhang et al. observed that hexoses (glucose, galactose, and mannose) required higher temperatures (110°C versus 100°C for pentoses) to achieve the same conversion as pentoses (xylose, and arabinose).[18] Using NiFe nanoparticles as catalysts, Ullah et al. observed higher conversions for xylose, mannose and rhamnose than for arabinose and galactose.[22] With Ru/Al_2O_3 catalyst, higher yields in polyols where obtained from xylose and fructose than for mannose and galactose at full conversion.[23] Simultaneous hydrogenation of galactose and arabinose was studied by Sifontes Herrera et al.[24] and Müller et al.[25] Both teams observed that arabinose hydrogenation was faster than galactose hydrogenation and estimated similar activation energies for arabinose and galactose; the former team assumed a negligible adsorption of galactose on Ru, whereas the latter team assumed a negligible adsorption of arabinose on Ru. Simultaneous hydrogenation of xylose, glucose and arabinose over Ru catalysts indicated a slightly slower rate of hydrogenation for glucose but this difference was sometimes negligible depending on the catalytic system.[26] In a different scope, Lari et al. observed that the combination of epimerisation and hydrogenation depends on the type of sugar, with higher reaction rate for arabinose, then glucose, then xylose, over Ru/C catalyst doped with Mo.[27]

Furthermore, the hydrogenation of sugars mixture produced by hydrolysis of hemicelluloses without purification has been investigated with Ni Raney catalyst on corn straw hydrolysates,[28] with ruthenium catalysts (hydrolysates from pure xylan,[29,30] sugarcane bagasse,[31] from birch[32] or from wheat bran[26]), or with bimetallic Ru-Ni catalysts (hydrolysates from sugarcane bagasse[33]). The presence of impurities such as furans or proteins can deactivate the catalyst.

Kinetic models have been proposed for sugars hydrogenation with catalysts such as Raney nickel catalyst,[34] Ru/C. Generally, the kinetics follow a Langmuir-Hinshelwood type mechanism, considering the competition between sugar and H_2 for the catalytic active site, but as far as we know, no adsorption studies have been carried out to measure the adsorption of the reactants and products. The desorption step of sugar alcohol was never considered in the literature. Kinetic modelling studies have generally been based on the hydrogenation of pure individual sugars or binary mixtures, and more rarely on the hydrogenation of hydrolysates of biomass: a Langmuir-Hinshelwood model has been used for the hydrogenation of sugars in biomass hydrolysates[31] and a pseudo-homogeneous first order model in two other studies.[30,33]

In the present paper, Ru/TiO_2 catalyst was prepared and applied to the hydrogenation of hemicellulosic sugars. The influence of reaction conditions was investigated for xylose hydrogenation and mass transfer limitations were estimated. A kinetic model based on Langmuir-Hinshelwood mechanism was designed and used to estimate kinetic parameters. The impact of sugar structure on initial reaction rate was investigated and discussed.

Results and Discussion

Catalyst preparation and characterisation

Ru/TiO_2 catalyst was prepared by incipient wetness impregnation followed by calcination under N_2 and reduction under H_2 and characterised by several techniques (Table S1 in ESI). The preparation and characterisation of Ru/TiO_2 catalysts was detailed in another publication from our group.[35] Briefly, characterisation results show that the catalyst is composed of nanoparticles of Ru°,

weakly dispersed on a TiO_2 rutile support with a very low surface area (non-porous material). Our previous results have shown that despite of the low dispersion of ruthenium, this catalytic formulation is suitable for highly selective hydrogenation.

Xylose hydrogenation with Ru/TiO_2

Xylose hydrogenation was performed in batch mode, at 120°C. Without catalyst, the thermal degradation of xylose was inferior to 10 % after 4 h. In the presence of Ru/TiO_2, xylose was completely converted after 2 h and xylitol was formed with a selectivity of ca. 100 % (Figure 1). For the sake of simplicity, Ii the following paragraphs the reaction advancement will be represented through xylose conversion only. Under our operating conditions, xylitol selectivity during xylose hydrogenation was always superior to 97% except when temperature was increased to 140°C (see below).

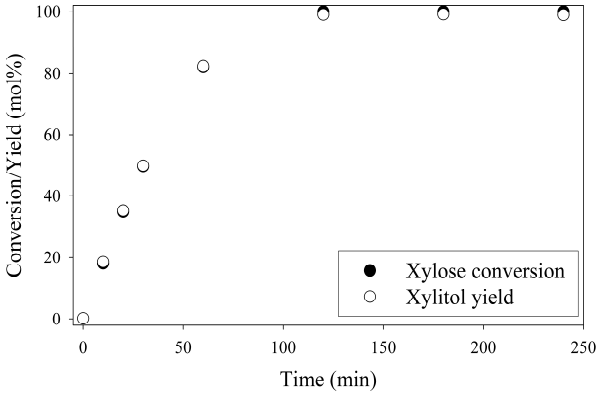

Figure 1. Xylose hydrogenation over Ru/TiO_2 catalyst. Reaction conditions: 120°C, 40 bar H_2, 0.33 M xylose, ratio Ru/xylose 0.45%, stirring rate 1600 rpm.

Influence of mass transfer limitations

The absence of external and internal mass transfer limitations in xylose hydrogenation over Ru/TiO_2 at 120°C, 40 bar was established by calculating Froude numbers and Weisz moduli (see ESI for details). This statement is valid for all the experimental conditions studied in this article: 80-120°C, 20-40 bar, catalyst concentration 5-15 $g.L^{-1}$.

Influence of reaction conditions in xylose hydrogenation

The influence of experimental conditions on xylose hydrogenation over Ru/TiO_2 was determined by varying each reaction parameter independently (Figure 2).

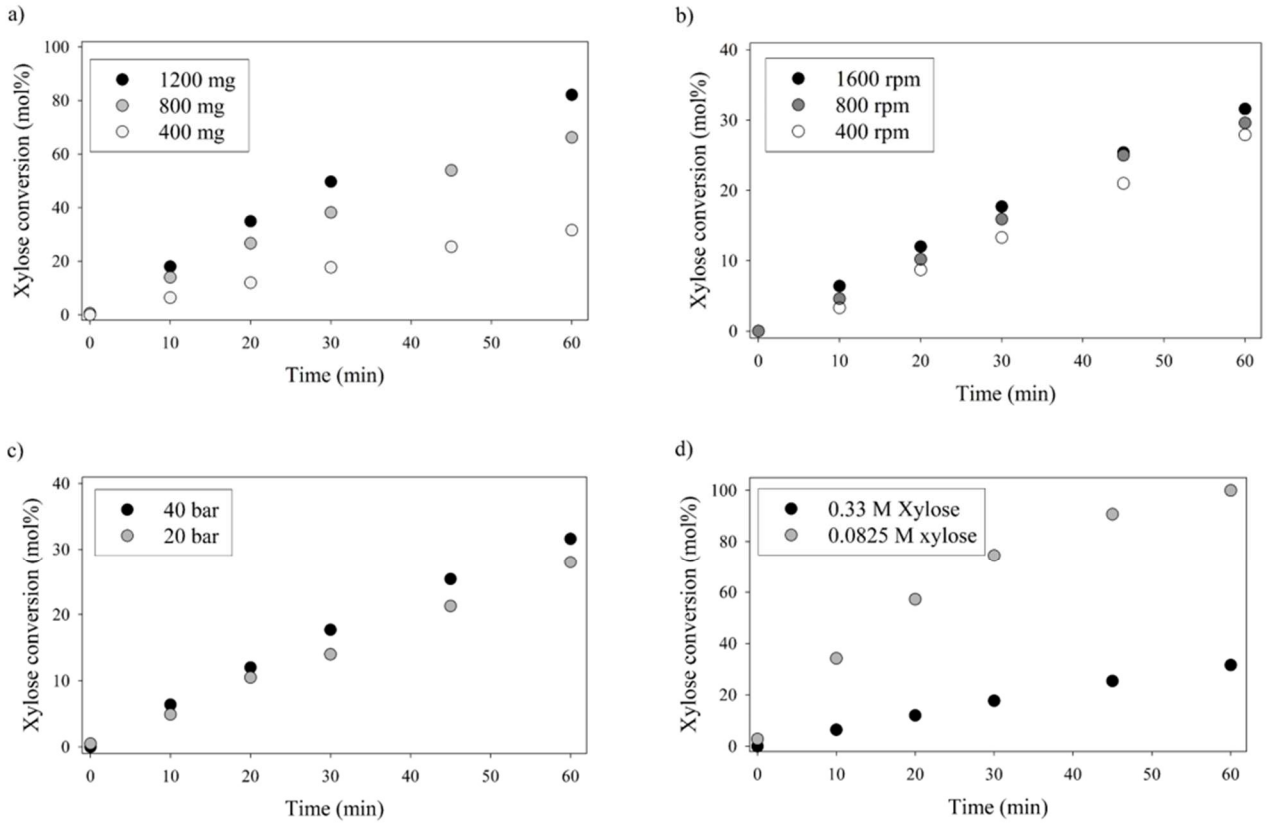

Figure 2. Influence of catalyst amount (a), stirring rate (b), H_2 pressure (c), xylose concentration (d) on xylose hydrogenation over Ru/TiO_2. Reaction conditions: 40 bar H_2, 0.33 M xylose, ratio Ru/xylose 0.15%, stirring rate 1600 rpm.

Mass of catalyst (Figure 2-a). Varying the catalyst amount from 400 mg to 1200 mg leads to a proportional variation in conversion rate and yield. As expected, there is a clear correlation between the amount of catalyst, i.e. the number of catalytic sites, and the rate of xylose hydrogenation in aqueous phase.

Stirring rate. Changing the stirring rate from 400 rpm to 1600 rpm led to a slight increase in the rate of xylose hydrogenation to xylitol, close to the uncertainty of measurement. Therefore, the experiment did not evidence a strong impact of stirring rate and thus of external mass transfer limitation at the gas-liquid interface nor at the solid-liquid interface. These results are consistent with the calculation of Froude numbers (see ESI), showing the absence of external mass transfer limitations.

Pressure of H_2. Reducing the pressure of H_2 from 40 bar to 20 bar did not influence the rate of xylose conversion, evidencing that hydrogen availability in aqueous phase is not a limiting factor in the reaction. The determination of Froude number for gas-liquid mass transfer at the corresponding pressures did not show any limitation of the reaction by hydrogen transfer from gas to liquid (see ESI).

Concentration of xylose. Decreasing xylose concentration at constant catalyst concentration (i.e. xylose/catalyst ratio was decreased) led to a drastic increase in xylose conversion rate.

Temperature. The effect of temperature was investigated between 80°C and 140°C. A significant increase in reaction rate (i.e. in rate of conversion) was observed when the temperature increased (Figure 3). At 140°C, the xylitol selectivity was only 88% at complete conversion (after 20 min) but was then stable for more than 3 hours, indicating that some by-products may be formed during xylose conversion at high temperature but xylitol itself is not degraded under our reaction conditions. The nature of by-products being formed remains unknown, as no additional peak was observed during HPLC analysis (see ESI, Fig S2).

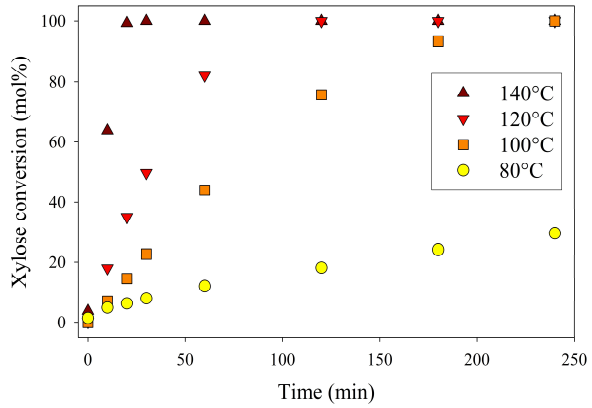

Figure 3. Influence of temperature on xylose hydrogenation over Ru/TiO_2. Reaction conditions: 40 bar H_2, 0.33 M xylose, ratio Ru/xylose 0.15%, stirring rate 1600 rpm.

Finally, the following parameters were applied for the rest of the study: mass of catalyst 400 mg, reaction time 4 h, stirring rate 1600 rpm and H_2 pressure 40 bar, temperature 120°C and sugar concentration 0.33 M. These reaction conditions guarantee a kinetic regime.

Kinetics of xylose hydrogenation

The experimental results were used to determine kinetics parameters for xylose hydrogenation over Ru/TiO_2. The experiments were carried out by varying the experimental conditions described in **Table 1**.

Table 1. Experimental parameters of xylose hydrogenation.

Parameter	Value
Number of experimental points	70 (6 or 8 per catalytic test)
m_{cata} - (0.77 %) Ru/TiO_2 (g)	0.4, 0.8, 1.2
Temperature (°C)	80, 100, 120, 140
Pressure (bar)	40
Liquid volume (L)	0.08
Initial solution	Pure xylose (0.08, 0.19, and 0.33 M) or xylitol (0.08 M) + xylose (0.33 M)
$C_{0,xylose}$ (mol.L^{-1})	0.08, 0.16, 0.33, 0.5
$C_{0,xylitol}$ (mol.L^{-1})	0 or 0.08

Mass balances. The reaction was assumed to be 100% selective with xylose as the only reactant and xylitol as the only product. The mass balance in the liquid phase is given by Equation (1):

$$\frac{dC_{Xy}}{d\tau} = -\frac{dC_{Xoh}}{d\tau} = -\frac{n_{Xy_0}}{V_L}.r = \frac{n_{Xoh_0}}{V_L}.r \quad (1)$$

where C_{Xy} and C_{Xoh} are the reactant and product concentrations, respectively, V_L is the liquid volume inside the reactor, and r is the reaction rate in $mol_{xylose}.mol_{Ru}^{-1}.min^{-1}$. τ stands for the contact time in $mol_{Ru}.min.mol_{xylose}^{-1}$, calculated using the number of ruthenium moles (n_{Ru}, in mol_{Ru}) the initial number of xylose moles ($n_{xylose0}$, in mol_{xylose}), and the reaction time t, as given by Equation (2):

$$\tau_1 = \frac{t.n_{Ru}}{n_{xylose_0}} \quad (2)$$

Hypothesis for modelling xylose hydrogenation. (i) The absence of internal and external limitations was verified (see above). (ii) The H_2 pressure did not influence the reaction rate during the experimental tests (see above) and the reactor was open in H_2. Therefore, H_2 concentration in water was assumed to be constant and equal to the concentration at thermodynamic equilibrium during the reaction. (iii) The reaction rate was assumed to follow the Arrhenius law.

Kinetic model. Based on these hypotheses and previous kinetic studies from literature, a Langmuir Hinshelwood formalism was considered to set the reaction rate. This rate equation suggests that a surface bimolecular reaction is the rate determining step with an adsorption competition between the sugar and the polyol adsorbed on the active sites of the catalyst. The absence of H_2 term in the denominator of the rate expression is justified according the literature where H_2 is founded to have little influence on the sugars

hydrogenation at high pressure (above 30 bar), presenting low adsorption constants[24] or even not being considered in the kinetic model.[25] For example, Sifontes Herrera et al. estimated K_{H2} for the galactose or arabinose hydrogenation at least 100 times lower than the adsorption constants found for sugars and polyols.[24] Finally, according to our experimental observation of no influence of partial pressure of H_2 on reaction rate (as already mentioned in the paper), we have assumed a zero-order for the numerator term in our kinetic rate expression. Consequently, seeking to improve the estimation of the kinetic parameters and considering the high pressure (40 bar) applied in our experiments, the following reaction rate was proposed. The xylose hydrogenation reaction rate was then defined by Equation (3):

$$r = \frac{k.K_{Xy}.C_{Xy}}{\left(1 + +K_{Xy}C_{Xy} + K_{Xoh}C_{Xo}\right)^2} \quad (3)$$

where *r* is the reaction rate, defined in $mol_{xylose}.mol_{Ru}^{-1}.min^{-1}$, K_{Xy} and K_{Xoh} are the adsorption equilibrium constants of xylose, and xylitol, respectively, and C_{Xy} and C_{Xoh} represent the concentrations of xylose and xylitol, respectively, in $mol.L^{-1}$.

The rate constant *k* follows the Arrhenius law, and the adsorption equilibrium constants follow the Van't Hoff equations. To decrease the correlation between the pre-exponential factor/adsorption constant and the activation energy/adsorption enthalpy, a reparametrisation of the Arrhenius and the Van't Hoff equations was applied [36], as defined by the Equation (4), which represents the Arrhenius equation:

$$k = k_{T_{ref}} exp\left[-\frac{E_a}{R}\left(\frac{1}{T} - \frac{1}{T_{ref}}\right)\right] \quad (4)$$

where k_{Tref} is the frequency factor at the reference temperature (T_{ref}) (mean value on the temperature range of this study). E_a is the activation energy in $kJ.mol^{-1}$. *T* is the temperature in K, and *R* stands for the universal gas constant (8.314 $J.K^{-1}.mol^{-1}$). k_0 is then calculated from k_{Tref} by the Equation (5):

$$k_{T_{ref}} = k_0 exp\left(-\frac{E_a}{RT_{ref}}\right) \quad (5)$$

The same reparametrisation was applied to adsorption constants following Van't Hoff equations.

Estimation of kinetic parameters. The estimated parameters are presented in Table 2. The estimated activation energy is in the same range of values as those found in the literature with different ruthenium catalysts.

Table 2. Estimated parameters for the xylose hydrogenation into xylitol kinetic model in batch mode.

Parameter	Value	Unit
k_{Tref}	22.37 ± 6.4 %	$mol_{xylose}.mol_{Ru}^{-1}.min^{-1}$
$K_{Xy,\ Tref}$	6.14 ± 14 %	$L.mol^{-1}$
$K_{Xoh,\ Tref}$	3.67 ± 18 %	$L.mol^{-1}$
ΔH_{Xy}	31.59 ± 66 %	$kJ.mol^{-1}$
ΔH_{Xoh}	1.45 ± 100 %	$kJ.mol^{-1}$
E_a	71.2 ± 21 %	$kJ.mol^{-1}$ (this work)
E_a [a]	*53.1*	*$kJ.mol^{-1}$* [37]
E_a [b]	*21*	*$kJ.mol^{-1}$* [17]
E_a [c]	*46.8*	*$kJ.mol^{-1}$* [38]

[a] Catalyst 3%Ru/carbon foam, 100-120°C (data from literature)

[b] Catalyst 5%Ru/C, 80-125°C (data from literature)

[c] Catalyst 1%Ru/zeolite HY, 100-140°C (data from literature)

The parity plot is presented in **Figure 4**, together with an example of model-experiment fit. The kinetic model presented a good fit to the experimental data (R^2 = 0.9818), being able to represent well the effect of the temperature on the conversion of xylose.

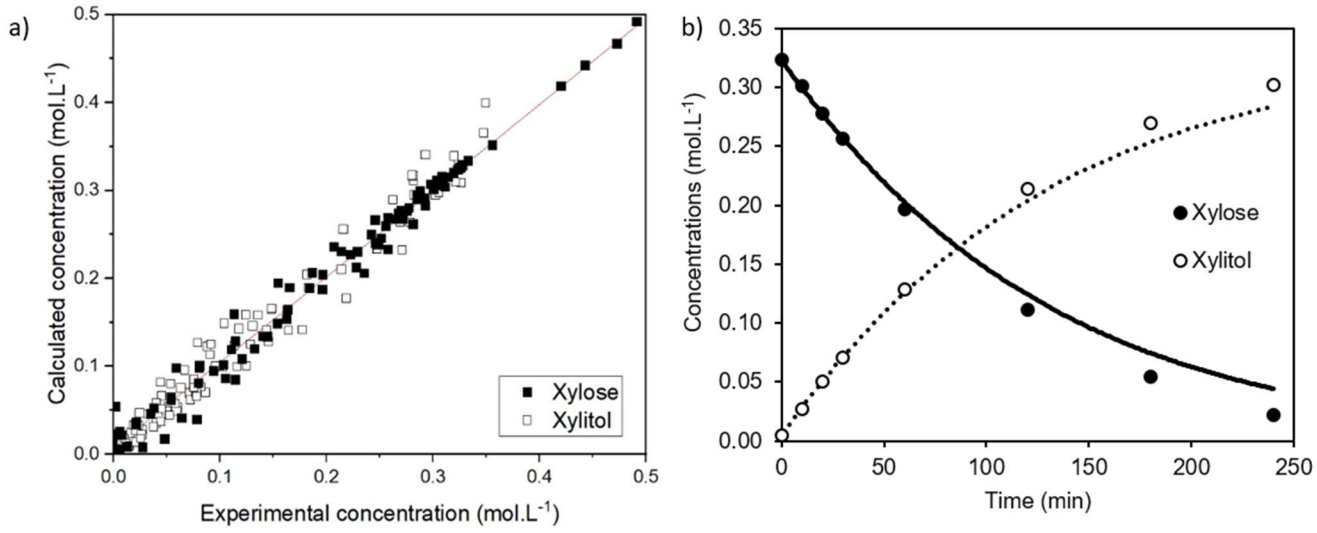

Figure 4. a) Parity plot of the experimental concentrations and the simulated concentrations. R^2 = 0.9833. b) Example of fitting experimental and calculated data. Reaction conditions: 40 bar H_2, 0.33 M xylose, ratio Ru/xylose 0.15%, stirring rate 1600 rpm.

The selectivity towards xylitol decreases with increasing temperature, suggesting increased by-products formation at high temperatures. This behaviour is observed at 140°C, where the selectivity reaches only 88% at long reaction times, compared to the 100% of selectivity towards xylitol at 120°C. This selectivity decrease is not taken into account in the model, thus leading to a drift in the modelled values at high temperature. It could be interesting to add a reaction to represent the formation of the by-products and therefore extending kinetic modelling to a larger range of temperature.

Effect of sugar type on the rate of hydrogenation reaction

Hemicellulose is a heteropolymer containing various pentoses and hexoses. The main sugars in its composition are xylose, arabinose (pentoses) and glucose, mannose, galactose (hexoses), all of which are aldoses, i.e. the unsaturated carbon is C1, forming alternatively a carbonyl C=O bond or an ether C-O-C bond depending on the conformation of the sugar.

Arabinose, glucose, mannose and galactose were hydrogenated individually under the experimental conditions previously optimised for xylose (Figure 5). Xylose reached 93 % conversion after 4 h, arabinose reached 90 % after 4 h with a conversion trend very similar to the one of xylose; glucose reached only 50 % conversion after 4 h, galactose 56 %, mannose 52 %, the three hexoses presenting similar curves of conversion. Each sugar produced only the corresponding polyol, namely xylitol, arabitol, sorbitol, mannitol, dulcitol (see Scheme 1). Surprisingly, the rate of conversion was correlated with the number of carbon atoms: arabinose and xylose were more than 50 % converted after 1 h whereas glucose, mannose and galactose reached 50 % conversion only after 4 h.

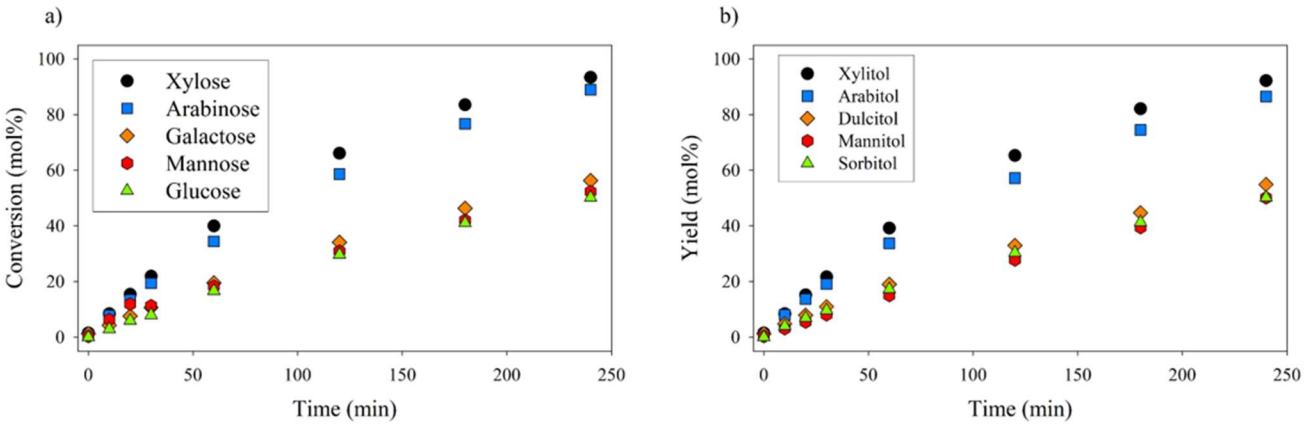

Figure 5. Hydrogenation of ex-hemicellulose sugars over Ru/TiO_2. Reaction conditions: 120°C, 40 bar H_2, 0.33 M sugar, ratio Ru/sugar 0.15%, stirring rate 1600 rpm.

Initial reaction rates were calculated from the linear regression of sugars concentration vs time at 120°C for 60 min and depicted on Figure 6. The highest initial reaction rate was obtained with xylose hydrogenation (238 $mol_{Xylose}.min^{-1}.mol_{Ru}^{-1}$). Initial rate of arabinose hydrogenation was only 85 % of this value; initial rates of glucose, galactose and mannose hydrogenations were only 42 %, 48 % and 53 % of xylose hydrogenation rate, respectively, demonstrating the impact of carbon atoms number on initial reaction rate but also, to a lesser extent, the role of stereochemistry of the sugars on hydrogenation. Indeed, arabinose and xylose differ only in the conformation of carbon n°4 and glucose, galactose and mannose differ only in the conformation of carbon n°4 (galactose) or n°2 (mannose).

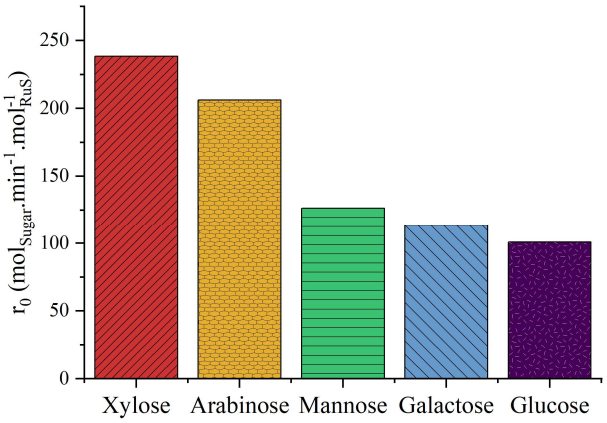

Figure 6. Initial reaction rate of sugars hydrogenation over Ru/TiO_2. Reaction conditions: 120°C, 40 bar H_2, 0.33 M sugar, ratio Ru/sugar 0.15%, stirring rate 1600 rpm.

Hydrogenation of sugars occurs through adsorption of sugar on Ru, H_2 dissociative adsorption on Ru, and H transfer to the sugar to form an -OH group. It should be noted that aldoses can adsorb as open-chain aldehydes or as pyranoside, so the new -OH group can be formed from a C=O group or from a C-O-C group. Therefore, several hypotheses can be made to explain the impact of sugar structure on hydrogenation rate:

i) The diffusion of sugars into the catalyst pores is the rate-limiting step, or
ii) The adsorption of sugar is the rate-limiting step and depends on the sugar structure, or
iii) The hydrogenation itself is the rate-limiting step and depends on the sugar structure.

Hypothesis i) can be disregarded when comparing xylose and glucose: their diffusion coefficients are very similar [39] and thus have very little impact on the Weisz-Prater modulus used to determine internal diffusion limitations. Indeed, the value of ϕ'_{xylose} is $9.3.10^{-5}$ (see ESI) and the value of $\phi'_{glucose}$ is $3.9.10^{-5}$, evidencing an absence of internal mass transfer resistance.

However, in cases ii) and iii), an impact of sugar structure in an open-chain form is improbable, since all aldoses would have very similar conformations with an aldehyde group at one end of the carbon chain and a primary -OH group at the other end. It is well known that in aqueous phase all the studied sugars are in large majority (>95%) present in pyranoside form at thermodynamic equilibrium (see ESI for details).[40] In pyranoside conformation, pento-aldoses and hexo-aldoses have different geometries: for the former ones,

all carbon atoms are included in 6 members-cycle, whereas for the latter ones, a -CH_2OH group is placed at the exterior of the cycle, in β position in relation to the ether bond, and could generate steric hindrance effects slowing down adsorption and/or hydrogenation steps. Further theoretical investigation (for example DFT calculation) would be necessary to support this hypothesis.

Conclusion

The hydrogenation of hemicellulose sugars over a solid Ru/TiO_2 catalyst was investigated. Hydrogenation of xylose resulted in the selective production of xylitol. The absence of internal or external mass transfer limitations was verified under the studied reaction conditions. The influence of several operating conditions was established: increasing the concentration of catalyst led to increase the reaction rate; stirring rate and H_2 pressure did not have a strong influence on reaction rate; increasing the temperature led to increase the reaction rate, without any impact on selectivity; increasing xylose concentration led to decrease reaction rate.
Kinetic modelling was used to determine the kinetic parameters for xylose. The proposed kinetic model followed a Langmuir-Hinshelwood mechanism and was able to predict the results obtained experimentally on the range 80 and 140°C and initial xylose concentrations between 0.08 and 0.33 M. The kinetic model included the competition between the reactants and the products for the active sites of the catalyst. Kinetic parameters were obtained. They allow a good fit between calculated and experimental data and are decorrelated, except for two sets of parameters. More experimental data (varying the initial concentration in xylose, and xylitol for example) could help to resolve this correlation. In addition, it would be interesting to measure experimentally the adsorption of reactants and products on the ruthenium surface to refine the kinetic model.
For the first time, a comparative study of hydrogenation of five sugars composing hemicelluloses was performed. We showed that sugar structure has a strong impact on hydrogenation rate over Ru/TiO_2: aldo-pentoses react 2 times faster than aldo-hexoses under identical reaction conditions. The presence of α-CH_2OH group outside the pyranoside ring for hexo-aldoses is suggested to be responsible for this difference in reaction rates. Further investigation is needed to clarify this point. This result is interesting for the development of future biorefinery processes where different types of sugars can be produced and transformed.

Experimental Section

Materials

Ruthenium (III) chloride ($RuCl_3 \cdot xH_2O$), titanium dioxide rutile and xylose were purchased from Sigma- Aldrich, arabinose, galactose, mannitol, arabitol were purchased from Alfa Aesar, xylitol, mannose, dulcitol, sorbitol, xylitol were purchased from Acros Organics, and glucose from Fischer Chemicals, with purity higher than 98%. All materials were used without further purification.

Catalyst preparation

The catalyst was prepared by incipient wetness impregnation. TiO_2 powder was dried 2 h at 120°C. The precursor solution was prepared using the retention volume of the support for ethanol and the amount of $RuCl_3 \cdot xH_2O$ necessary to obtain 1%Ru/TiO_2. The solution was added drop by drop to the dry support with a continuous manual stirring until the formation of a homogenous paste. Finally, the paste was dried overnight at 120°C and crushed afterward. The powder was calcined at 250°C under N_2 flow and reduced at 350°C under H_2 flow in a tubular oven.

Catalytic test

The catalytic hydrogenation of xylose was performed in a 120 mL Top Industrie autoclave batch reactor heated by a jacket and stirred with a Rushton turbine. The reactor is equipped with a gas cylinder and a continuous feed of H_2. 80 mL of 0.0825 to 0.33 M sugar solution and 400 to 1200 mg of catalyst (molar ratio Ru/sugar 0.15% to 0.45%) were introduced in the reactor, which was closed and purged with N_2 before heating to the reaction temperature. Time zero was determined as the moment when the reaction mixture reached the programmed temperature and the reactor was pressurized with 20 to 40 bar H_2. Samples were taken regularly through a sampling valve and filtered with 0.2 µm syringe filters.

Analytical methods

HPLC analysis was performed on a Shimadzu apparatus equipped with a RID detector and a Phenomenex Rezex RPM column at 80°C with pure filtered water as a mobile phase, 0.6 $mL.min^{-1}$. Additionally, a Phenomenex Rezex ROA column at 50°C with acidified water as mobile phase (0.005 N H_2SO_4) was used to confirm the identification of sugars and polyols by comparing the retention times of commercial standards. External calibration with four levels was used for quantification of sugars and polyols.

Sugars conversion and polyols yield at time t were calculated from molar concentrations as follows:

$$C_{Sugar}(mol\%) = \frac{[Sugar]_0 - [Sugar]_t}{[Sugar]_0} \times 100 \quad \text{and} \quad Y_{Polyol}(mol\%) = \frac{[Polyol]_t}{[Sugar]_0}$$

Concentrations at time = 0 came from the first sample taken at reaction temperature immediately after H_2 feeding.

Kinetic modelling tools

Xylose hydrogenation kinetics were modelled in MATLAB® R2020b. Kinetic parameters were estimated by non-linear data fitting, regressing the objective function, based on the sum of least-squares deviations between calculated and experimental data.

Electronic Supplementary Information

Catalyst characterization; calculations of mass transfer resistance; HPLC chromatograms; thermodynamic equilibrium of sugar forms.
Additional references cited within the Supporting Information:[39,41–46]

Acknowledgements

Stéphanie Pallier (CP2M), Laurent Veyre (CP2M), Ruben Vera (CDHL) and IRCELYON characterization platform are acknowledged for catalyst characterization. This project is funded by ANR grant CHICHE (ANR-18-CE43-0004). Marie-Line Zanota and Vincent Bernardin are thanked for their help on kinetic modelling.

Keywords: Arabinose • Galactose • Glucose • Hydrogenation • Langmuir Hinshelwood • Mannose • Ruthenium • Titanium dioxide • Xylose

[1] V. Schueler, S. Fuss, J. C. Steckel, U. Weddige, T. Beringer, *Environ. Res. Lett.* **2016**, *11*, 074026.
[2] W. Mauser, G. Klepper, F. Zabel, R. Delzeit, T. Hank, B. Putzenlechner, A. Calzadilla, *Nat. Commun.* **2015**, *6*, 8946.
[3] J. Philp, *N. Biotechnol.* **2018**, *40*, 11–19.
[4] A. T. Ubando, C. B. Felix, W.-H. Chen, *Bioresour. Technol.* **2020**, *299*, 122585.
[5] Y. Panchaksharam, P. Kiri, A. Bauen, C. vom Berg, Á. Puente, R. Chinthapalli, J. Spekreijse, J. Vos, S. Pfau, K. Rübberdt, J. Michels, L. König, *Roadmap for the Chemical Industry in Europe towards a Bioeconomy*, **2019**.
[6] S. V. Vassilev, D. Baxter, L. K. Andersen, C. G. Vassileva, T. J. Morgan, *Fuel* **2012**, *94*, 1–33.
[7] A. Ebringerová, Z. Hromádková, T. Heinze, in *Polysaccharides I* (Ed.: T. Heinze), Springer-Verlag, Berlin/Heidelberg, **2005**, pp. 1–67.
[8] H. V. Scheller, P. Ulvskov, *Annu. Rev. Plant Biol.* **2010**, *61*, 263–289.
[9] N. Sella Kapu, H. L. Trajano, *Biofuels, Bioprod. Biorefining* **2014**, *8*, 857–870.
[10] C. E. Wyman, S. R. Decker, M. E. Himmel, J. W. Brady, C. E. Skopec, L. Viikari, in *Polysaccharides* (Ed.: S. Dumitriu), Marcel Dekker, Inc., Hanover, New Hampshire, USA, **2005**, pp. 995–1033.
[11] P. Mäki-Arvela, T. Salmi, B. Holmbom, S. Willför, D. Y. Murzin, *Chem. Rev.* **2011**, *111*, 5638–5666.
[12] L. Vilcocq, P. C. Castilho, F. Carvalheiro, L. C. Duarte, *ChemSusChem* **2014**, *7*, 1010–1019.
[13] M. Grembecka, in *Encycl. Food Chem.* (Eds.: L. Melton, F. Shahidi, P.B.T.-E. of F.C. Varelis), Elsevier, Oxford, **2019**, pp. 265–275.
[14] Y. Delgado Arcaño, O. D. Valmaña García, D. Mandelli, W. A. Carvalho, L. A. Magalhães Pontes, *Catal. Today* **2020**, *344*, 2–14.
[15] T. Werpy, G. Petersen, *U.S. DoE Report DOE/GO-102004-1992* **2004**, *1*, 76.
[16] J. J. Bozell, G. R. Petersen, *Green Chem.* **2010**, *12*, 539.
[17] J. Wisniak, M. Hershkowitz, S. Stein, *Ind. Eng. Chem. Prod. Res. Dev.* **1974**, *13*, 232–236.
[18] X.-J. J. Zhang, H.-W. W. Li, W. Bin, B.-J. J. Dou, D.-S. S. Chen, X.-P. P. Cheng, M. Li, H.-Y. Y. Wang, K.-Q. Q. Chen, L.-Q. Q. Jin, Z.-Q. Q. Liu, Y.-G. G. Zheng, *J. Agric. Food Chem.* **2020**, *68*, 12393–12399.
[19] J. Lee, Y. Xu, G. W. Huber, *Appl. Catal. B Environ.* **2013**, *140–141*, 98–107.
[20] A. P. Tathod, P. L. Dhepe, *Green Chem.* **2014**, *16*, 4944–4954.
[21] M. Audemar, W. Ramdani, T. Junhui, A. Raluca Ifrim, A. Ungureanu, F. Jérôme, S. Royer, K. Oliveira Vigier, *ChemCatChem* **2020**, *12*, 1973–1978.
[22] N. Ullah, F. Jérôme, K. D. O. Vigier, *Mol. Catal.* **2022**, *529*, 112558.
[23] I. Bonnin, R. Méreau, T. Tassaing, F. Jérôme, K. De Oliveira Vigier, *ACS Sustain. Chem. Eng.* **2021**, *9*, 9240–9247.
[24] V. A. Sifontes Herrera, O. Oladele, K. Kordás, K. Eränen, J. P. Mikkola, D. Y. Murzin, T. Salmi, *J. Chem. Technol. Biotechnol.* **2011**, *86*, 658–668.
[25] A. Müller, G. Hilpmann, S. Haase, R. Lange, *Chem. Eng. Technol.* **2017**, *40*, 2113–2122.
[26] N. Sánchez-Bastardo, I. Delidovich, E. Alonso, *ACS Sustain. Chem. Eng.* **2018**, *6*, 11930–11938.
[27] G. M. Lari, O. G. Gröninger, Q. Li, C. Mondelli, N. López, J. Pérez-Ramírez, *ChemSusChem* **2016**, *9*, 3407–3418.
[28] A. Fehér, C. Fehér, M. Rozbach, G. Rácz, M. Fekete, L. Hegedűs, Z. Barta, *Chem. Eng. Technol.* **2018**, *41*, 496–503.
[29] G. Hilpmann, S. Steudler, M. M. Ayubi, A. Pospiech, T. Walther, T. Bley, R. Lange, *Catal. Letters* **2019**, *149*, 69–76.
[30] G. Hilpmann, P. Kurzhals, T. Reuter, M. M. Ayubi, *Front. Chem. Eng.* **2020**, *2*, DOI 10.3389/fceng.2020.600936.
[31] H. Baudel, C. de Abreu, C. Zaror, *J. Chem. Technol. Biotechnol.* **2005**, *80*, 230–233.
[32] X. Lu, P. Junghans, S. Weckesser, J. Wärnå, G. Hilpmann, R. Lange, H. Trajano, K. Eränen, L. Estel, S. Leveneur, H. Grénman, *Chem. Eng. Process. - Process Intensif.* **2021**, *169*, 108614.
[33] S. L. B. V. Carvalho, E. B. de Moraes Medeiros, A. de Souza Wanderley, L. de M. Ribeiro, J. G. da Silva, I. T. de Almeida Simões, N. C. do Rego Lemos, N. J. Ribeiro Neto, C. A. M. de Abreu, H. M. Baudel, N. M. de Lima Filho, *Chem. Eng. Res. Des.* **2021**, *174*, 11–18.
[34] J. Wisniak, M. Hershkowitz, R. Leibowitz, S. Stein, *Ind. Eng. Chem. Prod. Res. Dev.* **1974**, *13*, 75–79.
[35] L. Vilcocq, A. Paez, V. D. S. Freitas, L. Veyre, P. Fongarland, R. Philippe, *RSC Adv.* **2021**, *11*, 39387–39398.
[36] M. Schwaab, L. P. Lemos, J. C. Pinto, C. Pinto, *Chem. Eng. Sci.* **2008**, *63*, 2895–2906.
[37] T. N. Pham, A. Samikannu, A.-R. Rautio, K. L. Juhasz, Z. Konya, J. Wärnå, K. Kordas, J.-P. Mikkola, *Top. Catal.* **2016**, *59*, 1165–1177.
[38] D. K. Mishra, A. A. Dabbawala, J. S. Hwang, *J. Mol. Catal. A Chem.* **2013**, *376*, 63–70.
[39] N. Mogi, E. Sugai, Y. Fuse, T. Funazukuri, *J. Chem. Eng. Data* **2007**, *52*, 40–43.

[40] M. A. Kabayama, D. Patterson, *Can. J. Chem.* **1958**, *36*, 563–573.

[41] J. Wisniak, M. Hershkowitz, R. Leibowitz, S. Stein, *J. Chem. Eng. Data* **1974**, *19*, 247–249.

[42] V. Meille, N. Pestre, P. Fongarland, C. de Bellefon, *Ind. Eng. Chem. Res.* **2004**, *43*, 924–927.

[43] P. T. H. M. Verhallen, L. J. P. Oomen, A. J. J. M. v. d. Elsen, J. Kruger, J. M. H. Fortuin, *Chem. Eng. Sci.* **1984**, *39*, 1535–1541.

[44] P. Trambouze, J.-P. Euzen, *Chemical reactors : from design to operation*, Editions TECHNIP, Paris, **2004**.

[45] R. N. Goldberg, Y. B. Tewari, *J. Phys. Chem. Ref. Data* **1989**, *18*, 809–880.

[46] C. J. McGill, P. R. Westmoreland, *J. Phys. Chem. A* **2019**, *123*, 120–131.